Design and Development of a Capacitance Transducer for Airborne Particulates

Haroun Mahgerefteh and Styllianous Gerazounis
Department of Chemical Engineering
University College London
London WC1E 7JE

Abstract

The design and development of a co-axial capacitance transducer for on-line measurement of particulates in air is described. The system's performance is evaluated in response to changes in a number of operating parameters including relative humidity (8 - 78 %), temperature (20 - 100 ^{o}C) and flow velocity (6.5 - 15 m/s). Important particulate characteristics investigated include electrical properties, density, mean size and shape. It is found that the effective dielectric constant, ε_{eff} for all solids-gas dispersions tested is directly proportional to the solids concentration. However, in contrast to that for conducting powders, ε_{eff} for dispersions of insulating powders is found to be also dependent on the respective dielectric constant of the constituent solid particles, volumetric ratio as well as mean size. A 'temperature capacitor coefficient' is determined to account for the effect of temperature on the system's signal. Typical system particulate volumetric concentration resolution in the range 0 - 0.004% v/v is $\pm 2 \times 10^{-4}$ %.

1 Introduction

Black smoke released into the atmosphere by motor vehicles as well as industrial and house stacks is often the most obvious form of air pollution that is routinely encountered. The smoke is mainly composed of particulate matter; tiny solid or liquid particles in the range of 0.005 - 100 μm in diameter suspended in air (Baird, 1995). Recent studies have shown that such pollutants have a significant effect on human health [1] as well as the environment generally [2].

Particulates emitted by vehicles and more specifically from diesel-engined automobiles have attracted special attention due to their high contribution to the total particulate emissions (ca. 20%), high concentration, size distribution (they are within the respirable range), and chemical composition.

Monitoring particulates emitted from mobile sources is a difficult task due to a number of reasons. For example vehicular emissions contain particles with diameters varying from few nanometers up to several microns. Furthermore, the temperature of the exhaust gases is rather high and the exhaust flow is unsteady and non-uniform [3]. Nevertheless, because of its importance, the subject has attracted a great deal of attention in recent years leading to several particulate monitoring techniques with different degrees of sophistication.

The majority of the techniques so far developed are either expensive or their response is adversely affected by exhaust conditions other than particulate concentration. Few are capable of online operation.

In this paper we describe the preliminary design and development of an on-line particulate emission monitor aimed at overcoming most of the above problems.

Due to practical difficulties and safety implications associated with producing fine (<10 μm) particulate flows under controlled conditions, we study the system's performance in conjunction with relatively large particles (minimum 20 μm) only. Nevertheless, we envisage that our findings will be useful in assessing the potential of the proposed technology as a viable technique for use in practice.

2 Experimental

2.1 The capacitance transducer

Figure 1 is a schematic representation of a especially designed co-axial capacitor for maximising sensitivity. The unit comprises two conducting electrode tubes of different diameters placed coaxially so that an annulus is formed. A capacitor is created by application of a voltage, between the inner (1) (12 cm length, 1.8 cm dia.) and outer (2) (12 cm length, 3.24 cm dia.) electrodes. The relatively large ratio between the electrodes' length and separation distance (ca. 16) minimises capacitance fringe effects [4,5] which may otherwise result in non-uniform electric fields.

The electrodes are constructed from 0.2 mm thick, grade 316 stainless steel in order to minimise magnetic filed effects [6] and highly polished to prevent crono discharge [7]. Both ends of the inner electrode are fitted with hemispherical stainless steel (grade 316) caps (3). As well as avoiding corona discharge, the caps evenly direct and streamline the flow of particles through transducer’s annulus.

The inner tube electrode (1) is aligned parallel and central to the outer electrode (2) using three adjustable 12 BA metal screws (4) via Teflon sleeves (5) fitted to the outer electrode. The sleeves prevent the short-circuiting of the capacitor. Two spade connectors (6) fitted to the capacitance probe serve as the connection of the test leads via Kelvin clips to the LCR meter. One of these connectors is welded to the middle of the outside surface of the outer electrode (2) whilst the other is fitted to one of the three supporting screws (4) connected directly to the inner electrode. The transducer is securely attached to the powder conveying pipe via 4 mm wide Teflon rings (7) fitted on either side of the outer electrode (2).

The whole assembly is surrounded by a metallic earthed screen for guarding against interference from external electric fields. The relative humidity of the flowing stream is measured and controlled using an especially developed air humidifier [8] Full details of the particulate generation system constructed for the production of airborne particulates of various known concentrations under controlled ambient conditions are given elsewhere [8]. The system is capable of delivering particulate/air flow rates in the range 2 - 850 /min with a combined stability and reproducibly of ca. ± 4 %.

2.2 Materials

Bulk densities of particulates were measured using a pycnometer (AccuPyc 1330 Pycnometer, Micromeretics) with a claimed absolute precision of ± 0.01% of nominal full-

scale deflection. Particle size distributions were determined, with ca. ±3% precision using our recently developed vibro-spring particle sizing technique reported in an earlier study [9]. Dielectric constants on the other hand were obtained from the open literature [10].

3 Results and Discussion

3.1 Capacitance calibration curves

In the following, the performance of the capacitance transducer is evaluated by constructing 'capacitance calibration curves' for various solid-air dispersions comprising particulates of different dielectric (i.e. insulators and conductors) and physical properties (i.e. density, average particle size and shape) under various ambient conditions. These data are presented in the form of the variation of the effective dielectric constant of the solid-air dispersion, ε_{eff} plotted against the percentage solids volume fraction, f_S.

3.1.1 Insulating particulates

Figure 2 shows capacitance calibration data for suspensions of four different dielectric powders dispersed in air including amberlite, carbon black, soda glass ballotini and quartz. The average particle sizes, d_p vary in the range 20 -380 μm. As it may be observed, the dispersion effective dielectric constant, ε_{eff} is linearly proportional (correlation coefficient, C_c 0.992 - 0.996) to the concentration of solids drawn through the sensing volume. The fitting equation is given by:

$$\varepsilon_{eff} = K f_S + 1 \qquad (1)$$

The constant, K here termed as the dielectric proportionality constant, represents the rate of increase in, ε_{eff} with respect to the % solids volumetric concentration, f_S in the dispersion. Figure 2 indicates that, K increases with the solids dielectric constant (see table 1). Furthermore, when $f_S = 0$ (i.e. no suspended solids), ε_{eff} is equal to the dielectric constant of air which is unity. For a typical maximum deviation in ε_{eff} from linearly of $\pm 1 \times 10^{-3}$ and K = 5, the system sensitivity in monitoring solids volume fraction is $\pm 2 \times 10^{-4}$ % v/v.

Figure 3 shows the variation of the effective dielectric constant with % solids volume fraction for different volumetric ratios of quartz/glass mixtures. These experiments demonstrate the performance of the system in conjunction with particulate mixtures with different dielectric constants. As before, ε_{eff} increases in an approximately linear manner (C_c = 0.991 - 0.996) with the solids volume fraction, f_S. Furthermore, the mixture dielectric proportionality constant, K_{mix} (the slope of the fitted lines) increases with an increase in percentage volume of the constituent component with the higher dielectric constant, in this case glass balottini.

3.1.2 Conducting particulates

Figure 4 shows the variation of ε_{eff} with % solids volume fraction for various metal powder airborne particles including, bronze, copper and steel.

According to the data, ε_{eff} for all the systems tested obeys the characteristic equation (1), derived for dispersions of insulating powders. However, in this case a single calibration serves for all the powders tested. The fitting equation is given by:

$$\varepsilon_{eff} = 8.54 f_S + 1 \qquad (2)$$

3.1.3 The effect of particle size

Figure 5 shows the effect of particle size on the effective dielectric constant, ε_{eff} for various % volume concentrations, f_s of glass ballotini particulate-air dispersions. As expected the variation of ε_{eff} with f_s is approximately linear. Furthermore, for the same f_s, ε_{eff} decreases with decrease in the particle size. The latter observation is attributed to a decrease in electronic polarisation (the relative displacement of positive and negative charges) for smaller particles as a consequence of a reduction in the internal electric field inside them.

3.1.4 Effects of conveying air flow rate

The amount of static charge build-up due to triboelectrification depends on the degree of both particle/particle and particle/wall interactions. This raises an important question as to the effects of conveying flow velocity and the position of the capacitance transducer along the pneumatic pipeline relative to the feeding point on the measured capacitance.

Figure 6 shows the effect of the conveying air velocity on the effective dielectric constant for different volumetric fractions of glass ballotini (d_p = 90 μm) particulate-air dispersions. Based on the data, it is clear that within the ranges tested, for the same soilds volumetric fraction, the conveying air velocity has little effect on the data.

3.1.5 Effect of temperature

Figure 7 shows the effect of temperature plotted in the form of the variation of capacitance temperature shift ratio, ψ versus the mean air temperature, θ. ψ, is defined as

$$\varphi = \frac{C_{p(\theta)} - C_{p(\theta o)}}{C_{p(\theta)}} \qquad (3)$$

where $C_{P(\theta)}$ is the baseline capacitance (pF) at a mean temperature, θ. $C_{P(\theta o)}$ on the other hand is the corresponding capacitance value at a reference mean temperature, θ_o.

The mean temperature is given by

$$\theta = \frac{T_i + T_o}{2} \qquad (4)$$

where T_i and T_o are the inner and outer electrode surface temperatures (^oC), assumed to be equal to the flowing air and ambient temperatures respectively.

The data in figure 7 may be approximated by a straight line (C_c = 0.996) with the following capacitance temperature correction equation

$$C_{pair(\theta 2)} = C_{pair(\theta 1)}(1 + C_\theta \theta) \qquad (5)$$

where the slope of the fitted line, C_θ here defined as the capacitor temperature coefficient, is equal to 0.0001 $^oC^{-1}$. This value is surprisingly close the coefficient of linear expansion of the transducer's material of construction, stainless steel (c.f 0.00012 $^oC^{-1}$, Perry, 1973). Hence the observed increase in the baseline capacitance with temperature is attributed to the transducer's thermal expansion and not as a consequence of a change in the dielectric constant of air which at any rate is expected to be small and in the opposite direction [11].

3.1.6 Effect of Humidity

Tests involving the variation of the base line capacitance (the change in the base-line capacitance (no particulates) at a given humidity relative to the corresponding value at a 'dry' air relative humidity of 5%) indicate that this parameter remains relatively unchanged up to a relative humidity of ca 42%. Beyond this point, further increase in humidity results in a rapid and relatively linear increase in the shift in the baseline capacitance.

4 Conclusion

In this paper we presented the results of a series of experimental studies investigating the feasibility of operation of a coaxial capacitance transducer for the on-line monitoring of particulate concentrations in air. The effects of changes in a variety of parameters on the system's response were investigated. These included changes in particulate concentration, electrical properties, mean particle size, shape and flow rate as well as ambient temperature and relative humidity. The results indicate that the effective dielectric constant, ε_{eff} for all solids-gas dispersions tested is linearly proportional to the solids concentration. However, in contrast to that for conducting powders, ε_{eff} for dispersions of insulating powders is found to be also dependent on the dielectric constant of the particulates as well as their mean size. In the case of insulating particulate mixtures on the other hand, the rate of change in ε_{eff} with the total solids concentration increases in a linear manner with the volumetric ratio of the constituent particulate with the higher dielectric constant.

The observed decrease in the effective dielectric constant with a decrease in the mean particle size is attributed to a decrease in electronic polarisation inside the smaller particles. Electronic polarisation is acquired following static charge build-up due to triboelectrification of the test particles. In general it is found that such size dependency may be accounted for in terms of the electric susceptibility of the test particulates. Irregularity of the particles on the other hand is manifested in a slight increase in the internal field resulting in non-linear signal.

Experiments at various air humidities indicate that the systems response is essentially unaffected by air humidity up to ca. 40% following which further increase in humidity results in a rapid increase in the recorded capacitance.

The variation of the capacitor's signal with ambient temperature on the other hand is a consequence of the thermal expansion of the transducer material of construction.

5 References

[1] Baird, C., "Environmental Chemistry", W.H. Freeman & Co., New York (1995).

[2] Elsom, D.M., "Atmospheric Pollution: A Global Problem", Blackwell Publishers, London (1992).

[3] Harrison, M.R. and R. Perry, "Handbook of Air Pollution Analysis", Chapman and Hall Ltd., New York (1986).

[4] Scaife, B.K.P., "Principles of Dielectrics", Oxford Science Publications, Oxford (1989).

[5] Jonassen, N., "Electrostatics", International Thomson Publishing, New York (1998).
[6] Lockhart, N.C. and J.W. Snaith, "Apparatus for Dielectric Measurement on Fluids and Dispersions", Journal of Physics E: Scientific Instruments, **11**, 1011 (1978).
[7] Von Hippel A., "Dielectric Materials and Applications", Artech House, London (1995).
[8] Gerazounis, S., Nonel Particlute On-line Monitor, University College London PhD thesis, 2002.
[9] Mahgerefteh, H., A. Shaeri, "Modelling of a Novel Vibro-spring Particle Sizer, AIChE Journal, **47**(3), 562 (2001).
[10] Perry, R.H., and C.H. Chilton, "Chemical Engineers' Handbook", McGraw- Hill, New York, 5th Ed., 10-10 to 10-12 (1973).
[11] van Vlack, L.H., "Elements of Materials Science and Engineering", Addison-Wesley Publishing Company, New York (1989).

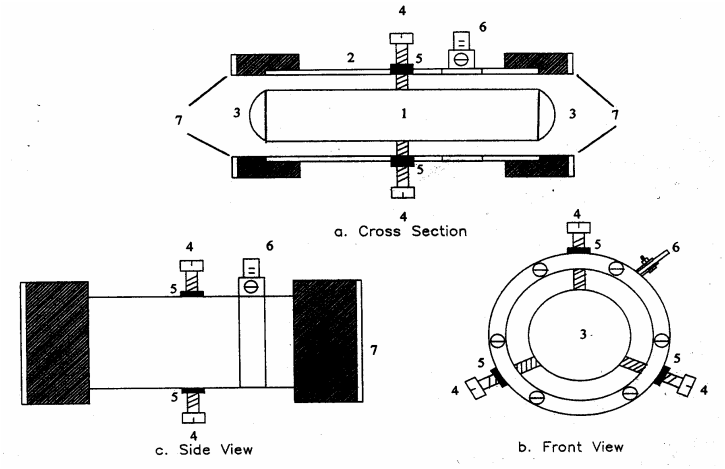

Figure 1. Various section views of the capacitance transducer (see text for details)

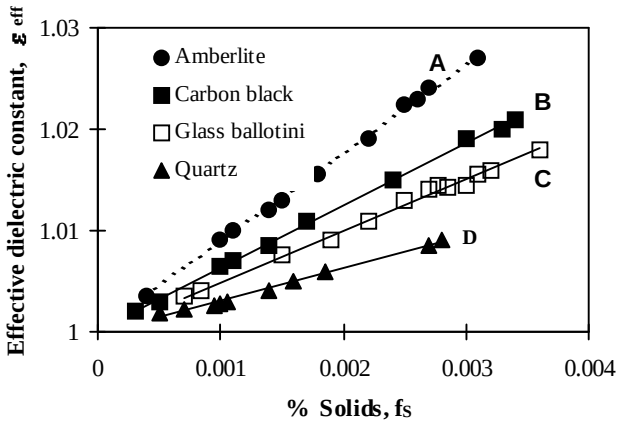

Figure 2. The variation of effective dielectric constant, ε_{eff} with % solids volume fraction, f_s for various insulating particulate-air dispersions.

Curve A: Amberlite, Curve B: Carbon black, Curve C: Glass ballotini, Curve D: Quartz.

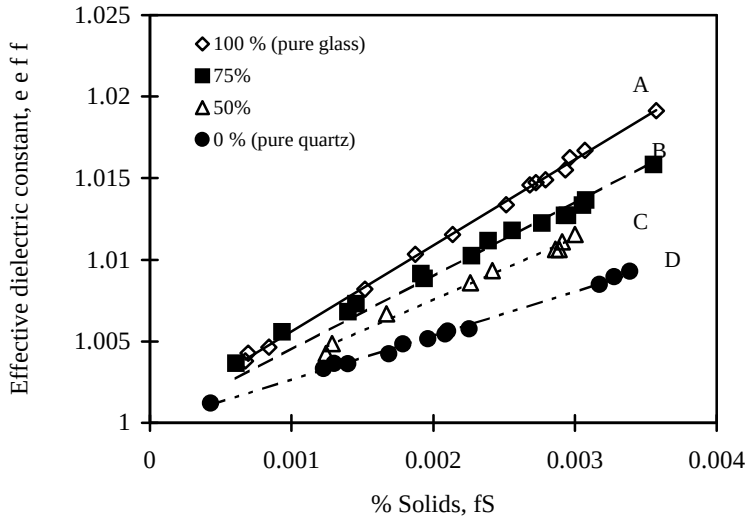

Figure 3. The variation of effective dielectric constant, ε_{eff} with % solids volume fraction, f_s for different volumetric ratios of quartz/glass particulate-air dispersions.
Curve A: 100 % glass ballotini; Curve B: 75 % glass ballotini; Curve C: 50 % glass ballotini; Curve D: 100 % quartz.

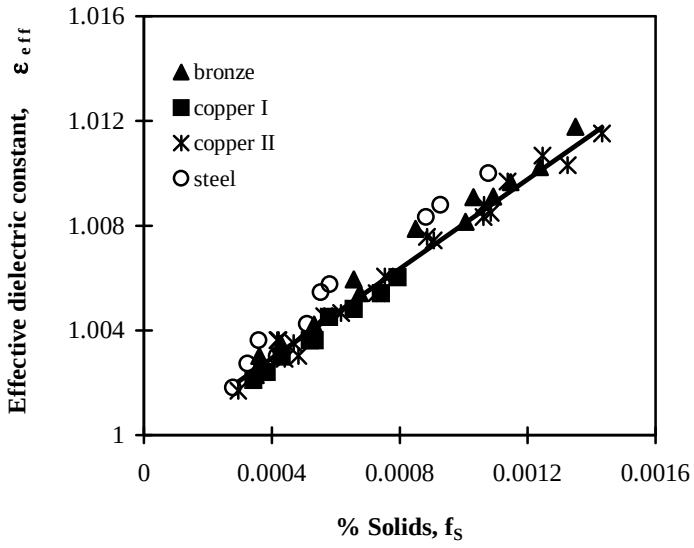

Figure 4. The variation of effective dielectric constant, ε_{eff} with % solids volume fraction, f_s for various conductive particulate/air dispersions.

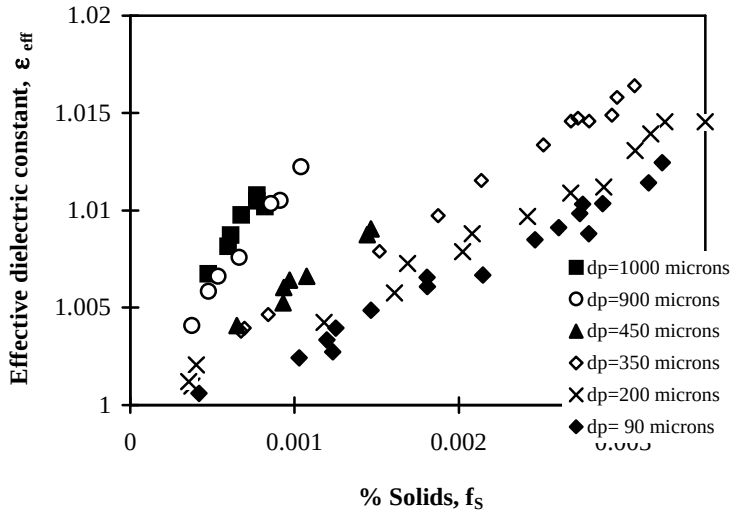

Figure 5. Effect of the particle size, d_p on the effective dielectric constant, ε_{eff} for various solids volumetric fractions of glass ballotini particulate/air dispersions.

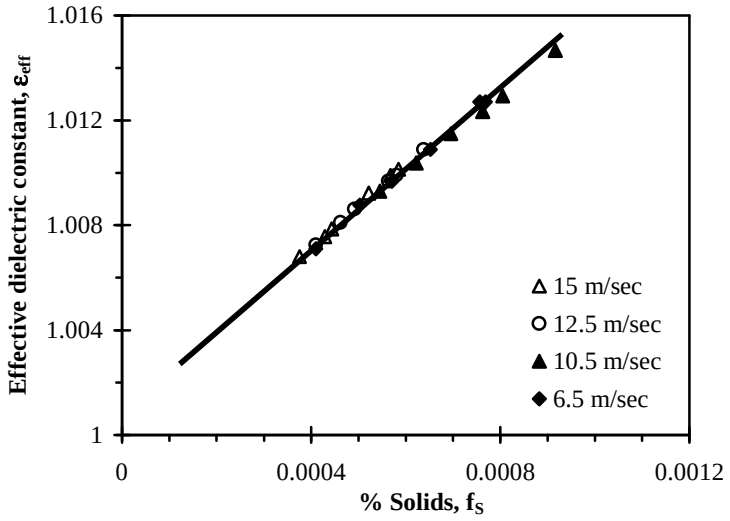

Figure 6. The variation of effective dielectric constant, ε_{eff} with solids volume fraction, f_S for glass ballotini (d_p = 90 μm) particulate-air dispersions at various conveying air velocities.

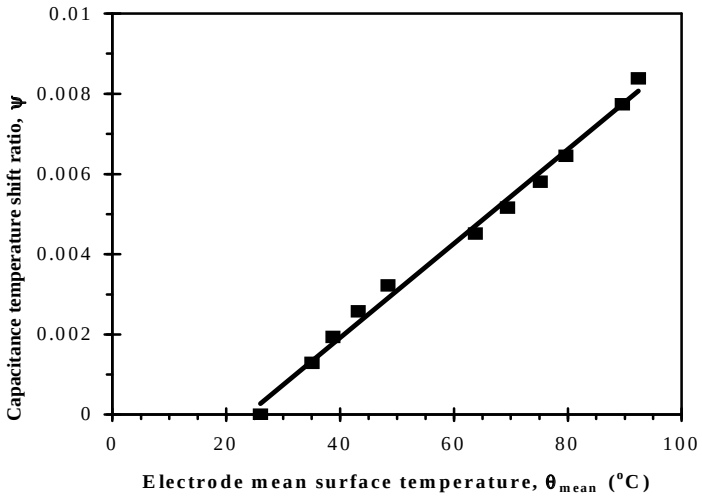

Figure 7. The variation of the fractional change in capacitance temperature shift ratio, ψ with electrode mean surface temperature, θ_{mean}.